

A Humidity Generator for Temperatures to 200 °C and Pressures to 1.6 MPa

D. Vega-Maza¹, W. W. Miller², D. C. Ripple^{2,3}, and G. E. Scace²

¹University of Valladolid, Valladolid, Spain

²Process Measurements Division, National Institute of Standards and Technology, Gaithersburg, MD 20899, USA

³ To whom correspondence should be addressed. E-mail: dean.ripple@nist.gov

Official contribution of the National Institute of Standards and Technology; not subject to copyright in the United States.

Abstract

We have constructed a new humidity generator that produces gas streams of known moisture content at temperatures from 85 °C to 200 °C, absolute pressures from 0.2 MPa to 1.6 MPa, and relative humidities from 10 % to 90 %. The generator produces a moist gas stream by injecting fixed-rate streams of dry gas and liquid water into a vaporizer, where the water evaporates into the gas. The gas stream passes into a re-entrant radio-frequency (RF) cavity, which serves as our reference hygrometer, and then a test chamber. The present standard uncertainty of the RF hygrometer is 0.6 %, limited by the uncertainty of literature values for the polarizability of water. Dry nitrogen gas purging the pressure transducer line also combines with the moist gas stream downstream of the test chamber and flows through one of a set of capillaries. Modulation of gas flow through the fixed flow impedance of the capillary gives a simple method for controlling pressure. Individual insulated, temperature-controlled aluminum ovens enclose each major component. A larger oven encloses these ovens and their connecting tubing. To minimize corrosion, critical components are constructed of high-nickel alloys. The small total volume (< 1 L) and small flow rate (<0.5 L/min) reduce operational hazards from steam scalding or from gas explosion.

Keywords: fuel cell, humidity, humidity generator, steam, water

1 Introduction

A number of specialized processes, such as optimal humidification of fuel-cell feed gases, require measurement and control of humidity at temperatures or dew points well in excess of 100 °C [1]. In support of these processes, we have constructed a new humidity generator that produces gas streams of known moisture content at temperatures from 85 °C to 200 °C, absolute pressures from 0.2 MPa to 1.6 MPa, and relative humidities from 10 % to 90 %. Traditionally, generators of humid gas streams have saturated a dry gas stream at known temperature and pressure, and then reduced the moisture level below saturation by either raising the gas temperature, or expanding the gas to a lower pressure, or a combination of both. The resulting gas stream has a known moisture content. Such a generator becomes a primary standard if a) temperature and pressure are measured accurately, and b) the saturated vapor pressure of water and corrections for gas non-ideality (the enhancement factor) are known.

The necessary thermodynamic properties of water substance [2] are known at sufficiently low uncertainties to enable construction of a thermodynamically based humidity generator for operation at temperatures above 100 °C. However, we did not pursue this approach for several reasons:

1. Ensuring full gas saturation requires a relatively large saturator. We wished to minimize the saturator volume to allow operation with potentially explosive gas mixtures (e.g., moist hydrogen).
2. Thermodynamically based generators require that the saturator be maintained at a uniform and stable temperature. For the potentially broad range of desired saturator temperatures (50 °C to 200 °C), maintaining temperature uniformity and stability would require either a large oil bath or a multi-shell furnace.

We chose to take an alternate approach to creating a humidity standard by using a stable, calibrated hygrometer to characterize the moisture content of a gas stream produced by a repeatable, but not primary, humidity generator. Our previous work with an RF-resonator hygrometer [3] over the temperature range 42 °C to 84 °C demonstrated that the instrument is robust, fast, and repeatable. The RF resonator hygrometer detects moisture concentration by measuring the shift in an electromagnetic resonance induced by shifts in the gas dielectric constant. For the elevated temperature and pressures anticipated for this generator, the shifts in dielectric constant are much larger than observed in our previous work, and we anticipated having excellent signal to noise for this application.

2 Design of the Generator

2.1 General Principles of Operation

We described the principles of the RF resonator in previous publications [3] and give an overview in section 2.2. In section 2.3, we focus on the design of the generator, which incorporates the RF resonator hygrometer as one of its elements. Figure 1 shows a schematic diagram of the generator.

In concept, the operation of the generator is simple. Separate, metered streams of dry gas and liquid water are combined in an elevated-temperature vaporizer. The flow of dry gas is controlled by a mass flow controller, and the flow of liquid water is controlled by a chromatography pump and back-pressure regulator. In the vaporizer, the water turns to steam and mixes with the dry gas. The combined gas stream passes through an RF-resonator hygrometer, and then through a test chamber where test hygrometers may be mounted. Downstream of the test chamber, a high flow-impedance valve or one of several capillary

tubes restricts the flow, thereby maintaining an operating pressure greater than ambient pressure.

In practice, there are several challenges. First, high-temperature, distilled-water steam can be highly corrosive. We tested several alloys for resistance to steam and water exposure at 200 °C by placing samples of different alloys and distilled water in a sealed container and then heating to 200 °C for up to 7 days. After this period, we visually inspected the alloy samples and had the water chemically analyzed. Inconel 600* and Hastelloy C-22* proved highly resistant; 316L stainless steel also appeared suitable, although anecdotal experience suggests 316L may suffer corrosion after extended use. Guided by these results, we fabricated the major components of the generator from Inconel 600 tubing and plate whenever possible. To avoid corrosion of embedded particles from high-speed steel cutting tools, carbide cutting tools were used throughout for machining and facing connecting tubing. Suitable Inconel 600 tube fittings to assemble the components could not be found, so we used Hastelloy fittings designed for gas chromatography use. To develop a pressure head, we used a needle valve or small-bore capillary tubing. Neither the valve nor the capillary tubing could be obtained in Inconel 600 or Hastelloy. Consequently, we used 316L stainless steel for these components. Because these valves and tubing are all downstream of the test chamber and RF resonator, any corrosion developed over long use will not lead to contamination or measurement errors.

The second challenge was developing a simple method of measuring the gas pressure of a gas stream with a dew point much greater than ambient temperature. A second mass-flow controller bleeds a stream of dry gas through the pressure port, preventing water condensation (and possible blockage) in the pressure line. The flow of gas through the pressure-port tube (2.4 mm inner diameter) caused a small pressure head. We estimated this pressure head by calculating the pressure drop at conditions of maximum volumetric flow ($1.7 \times 10^{-6} \text{ m}^3 \cdot \text{s}^{-1}$) using the Darcy-Weisbach Equation, with Darcy's friction factor from the Moody's diagram of 0.015, as appropriate for turbulent flow [4]. The pressure head along the tube induced by the flow was 100 Pa or less, which is negligible compared to the pressure gage uncertainty.

The purge flow for the pressure gauge also provides a very convenient method of controlling the operating pressure of the generator. For a fixed choice of capillary, the mass flow rate of the mixture of purge gas and moist gas is related to the pressure drop across the capillary by [5]:

$$Q_m = \frac{\pi r^4}{16\eta RT_c L} (P_1^2 - P_0^2) , \quad (1)$$

where Q_m is the mass flow rate, r is the inner radius of the capillary tube, η is the viscosity, R is the gas constant, L is the length of the capillary, T_c is the temperature of the capillary, P_1 is the pressure at the capillary entrance, and P_0 is the pressure at the capillary exit. Equation 1 demonstrates that as Q_m is increased by increasing the purge rate, the operating pressure P_1 increases as well. Our system has the capability of closed-loop pressure control, in which a proportional-integral-differential (PID) controller adjusts the purge-gas flow rate to stabilize the operating pressure.

The operating pressure of the generator may vary by a factor of almost 20, from ambient (0.1 MPa) to approximately 1.6 MPa (the saturated vapor pressure of water at 200 °C is 1.55

* Certain commercial equipment, instruments, or materials are identified in this document. Such identification does not imply recommendation or endorsement by the National Institute of Standards and Technology, nor does it imply that the products identified are necessarily the best available for the purpose.

MPa). By equipping the system with a set of six capillaries with different lengths (ranging from 0.18 m to 1.45 m) and bores (0.13 mm and 0.25 mm), a capillary can be chosen to match the desired operating pressure. By shutting off all other flow paths, gas flow is directed through one of the capillaries or the needle valve. We did not find a small shut-off valve that would give reliable operation at 200 °C in steam and could be actuated from outside the oven. As an alternative, all of the capillary and needle valve lines first transition to a stainless steel tube of 7.7 cm inner diameter, which is large enough that condensate cannot form a water bridge across the tube. These large tubes exit the furnace pointed down at an angle to allow condensation to drain, and are terminated at room temperature with valves with 7.1 mm orifices. Operation with the set of capillaries chosen for the present paper limits operation to a minimum absolute pressure of 0.2 MPa; with a capillary of lower flow impedance, control at pressures slightly above ambient pressure (0.1 MPa) should be possible.

From the vaporizer through the flow impedance elements, the system must be maintained at a temperature exceeding the dew point of the gas stream. This task could be accomplished by immersing the whole assembly in an oil bath, but that would risk contamination of the system and tested hygrometers. We chose to control the temperature by placing the components in two ovens: an auxiliary oven to contain the test chamber, and a main oven to contain all the other components. Each of the major components (vaporizer, RF resonator, test chamber, and flow impedance lines) were in turn encased in temperature-controlled aluminum housings. The gas stream entering the RF resonator and the test chamber is brought to thermal equilibrium with the aluminum housings in separate heat exchangers consisting of spiral of 3.2 mm outer diameter tubing, 0.53 m long, captured between aluminum plates bolted to the aluminum housings. A PID controller sensing a type K thermocouple and driving a flexible-sheet heater with DC voltage maintains each housing at a fixed temperature. A layer of microporous silica insulation, approximately 1 cm thick, surrounds each housing, limiting heat losses and reducing thermal non-uniformity of the housings to approximately 0.2 °C or less, for a housing temperature 10 K hotter than the surrounding oven.

2.2 RF Resonator Hygrometer

The resonance frequency of the RF resonator is a function of the dielectric constant of the gas stream. Relating the dielectric constant to water concentration, in turn, requires knowledge of:

1. Virial coefficients of the gas mixture,
2. Polarizability of the molecular species present in the gas mixture, and
3. Gas temperature and pressure.

The dielectric constant of a mixture of nitrogen gas and water vapor is related to other parameters by the expression [6]:

$$s(\varepsilon') = \frac{\varepsilon' - 1}{\varepsilon' + 2} = \frac{P}{RT(1 + B_{\text{mix}}P/(RT))} [(1 - x_w)A_n + x_w(A_w + B_w/T)] \quad , \quad (2)$$

where ε' is the real part of the complex dielectric constant $\varepsilon = \varepsilon' - i\varepsilon''$, P is the pressure, R is the gas constant, T is temperature, B_{mix} is the second virial coefficient of the gas mixture, x_w is the mole fraction of water, A_n is the polarizability of nitrogen, and A_w and B_w are the Debye constants describing the polarizability of water.

Equation (2) may be rearranged to obtain the equation relating x_w to all other quantities:

$$x_w = \frac{1}{(A_w + B_w/T) - A_n} [sRT/P + sB_{\text{mix}} - A_n] \quad , \quad (3)$$

P and T are directly measured quantities. We obtain ε' , and thus the parameter s , by measuring the shift in the center frequency, f , of the RF resonance in the moist gas, relative to

the frequency measured when the resonator is filled with dry nitrogen. We used a network analyzer to measure the transmission through the resonator as a function of frequency, and then fit the data to obtain f (see Ref. [3] for details). The polarizability A_n and Debye constants A_w and B_w were obtained from the literature [7,8,9]. The second virial coefficient is calculated from the equation [10]

$$B_{\text{mix}} = x_w^2 B_{\text{ww}} + 2x_w(1-x_w)B_{\text{nw}} + B_{\text{nn}}(1-x_w)^2, \quad (4)$$

using literature values for the second virial coefficient B_{nn} for nitrogen [10], B_{ww} for water [11], and B_{nw} for nitrogen-water interactions [12].

2.3 Additional Instrumentation

A NIST-calibrated 100 Ω platinum resistance thermometer inserted into a well in the resonator body measures the temperature of the RF resonator. We chose a model designed to have low thermal hysteresis, which was confirmed by an observed repeatability at the ice point of 0.02 $^{\circ}\text{C}$ after cycling to 200 $^{\circ}\text{C}$. A calibrated digital multimeter measures the resistance of the thermometer. The combined standard uncertainty of the temperature measurement is 0.02 $^{\circ}\text{C}$. We monitor the temperature of the test chamber, shown in Fig. 1, in a similar manner. (Further details of the test chamber and its performance will be given in a future publication.)

A strain-gauge based pressure transducer, calibrated against a deadweight pressure standard, measures the pressure of the gas in both the RF resonator and the test chamber. The standard uncertainty of the pressure readings varies from 0.05 kPa near 100 kPa pressure to 0.10 kPa at 2 MPa.

3 Operation of the Generator

The vaporizer in this generator functions completely differently than a saturator in a traditional generator. There are two modes of operation. In the first mode, we maintain the vaporizer at a temperature above the dew point, but below the bubble point (at the operating pressure). Liquid water will pass from the feed line into the vaporizer. We surmise that a puddle of water will collect in the bottom of the vaporizer. The puddle will grow until the evaporation from the puddle surface just balances the feed rate of the incoming water. In this mode, we attained pressure standard deviations of 20 Pa over a 10 min window and 120 Pa over 30 min, at operating pressures of 500 kPa. A minor drawback of this mode is that the humidity concentration does not reach steady state until a period of approximately 2 h.

Figure 2 shows that 120 min after a minor variation in set point (at time zero), the humidity concentration was stable to within 0.55 % of x_w , as indicated by the RF resonator. Figure 3 shows the fit of a resonance function to typical data, along with the residuals. The residuals have no discernible structure, consistent with our experience with this resonator at lower temperatures[3]. When the resonator was accidentally operated at a temperature below the gas dew point, the quality of the fit degraded very noticeably due to the presence of water droplets inside the resonator.

In the second mode of operation, we maintain the vaporizer at a temperature above the boiling point. In this case, the water may vaporize in the feed tube and enter the vaporizer as steam, or the water may enter as liquid and rapidly boil on the lower surface of the vaporizer. Equilibration in this mode is much more rapid. Unfortunately, the pressure in the system undergoes periodic oscillations, with a typical amplitude of 10 kPa and a period of 2 min to 5 min. Temperature measurements using thermocouples mounted on the feed tube confirmed that the tube-wall temperature oscillated with the same period. We explored a variety of operating conditions in an attempt to eliminate these oscillations, without significant success.

If vaporization was performed in an ebulliometer external to the main oven, the vaporizer could be fed from a continuous vapor stream, and the oscillations perhaps would be eliminated.

Adjustment of the purge rate through the pressure line proved to be a very easy method of controlling the operating pressure. In fact, because the significant gas volumes in the system (vaporizer, RF resonator, and test chamber) and the flow impedance (capillaries and needle valve) are all temperature controlled to within 0.02 °C, the pressure maintained a steady value without use of the PID pressure-control capability.

4 Uncertainty

Because the generator relies on the readings of the RF hygrometer to determine the mole fraction of water produced by the generator, the uncertainty in x_w can be no smaller than the measurement uncertainty of the RF resonator hygrometer.

We used Eq. 3 to obtain the combined uncertainty propagating from uncertainties of measured and calculated properties. The Debye constants were taken as the average of four sets of literature values of A_w and B_w that were determined over temperature spans of at least 70 K [9]; the standard deviation of the values of $A_w + B_w/T$ at 200 °C was 0.59 %. We took this standard deviation as the standard uncertainty for the polarizability of water, and this component proved to be the dominant uncertainty.

Figure 4 shows the combined and component uncertainties (all as standard uncertainties with coverage factor $k = 1$) for the sample case of resonator temperature of 200 °C and an operating pressure of 1.6 MPa. Table 1 gives the uncertainties of the parameters used to generate Fig. 4. From the figure, the uncertainty of the Debye constants clearly dominates the combined uncertainty. The temperature and the second virial coefficient of the mixture make small contributions to the uncertainty. Note that the very high relative uncertainty of B_{nw} does not contribute significantly because B_{nw} is small relative to both B_{nn} and B_{ww} at this particular temperature. Higher order virial coefficients are negligible. At lower operating pressures, the contribution of the second virial coefficient will drop, approximately linearly with pressure.

The combined standard uncertainty of 0.6 % could be reduced if we knew the Debye constants to better accuracy. We plan to calibrate our RF resonator, while installed in the generator, using a gravimetric method. We will measure the flow of dry nitrogen into the generator using a laminar flow element placed upstream of the generator. The mass flow of water will be measured by dynamically weighing the water container feeding the water pump. A calibration using this technique will give an in situ measurement of the value of $A_w + B_w/T$ and will greatly reduce the uncertainty contribution due to temperature non-uniformity of the RF resonator. The uncertainty will still be limited by the repeatability of the generator (including effects of variations in water vaporization and mixing, temperature variations, and pressure variations), by the uncertainty of the second virial coefficient of the gas mixture, and by the uncertainty of the gravimetric calibration.

The variation in humidity output of the generator, as seen in Fig. 2, does not contribute to the overall generator uncertainty provided that this variation in RF resonator readings reflects true changes in the moisture content of the gas. Gravimetric calibration measurements will be necessary to see if this is the case.

In addition to the calibration of the RF resonator, we need to perform measurements with P and x_w fixed while the temperature of the RF resonator is varied. These measurements will reveal any effects of water adsorption on the walls of the RF resonator as the temperature is reduced to a value near the dew point.

5. Conclusion

The generator we have developed demonstrates a simple, compact method to produce moist gas streams at elevated temperatures and pressures. Inserting the RF resonator for the measurement of water mole fraction into the flow path to the test chamber worked well, as did the temperature-controlled capillaries used as a pressure regulator. Routine operation of the generator as a standard for calibrations and research awaits completion of the gravimetric measurements. We are also considering whether to modify how the water is vaporized, in order to reduce the pressure oscillations when the vaporizer temperature is above the boiling point.

Acknowledgments

We thank Peter Huang and Allan Harvey for helpful advice and providing values of water-nitrogen virial coefficients prior to publication. One of us (David Vega Maza) gratefully acknowledges the grant from the Spanish Ministry of Research and Innovation and the European Union, reference ENE2006-13349/CON, which made participation in this research possible. This work was supported in part by the Advanced Technology Program of the National Institute of Standards and Technology.

Nomenclature

A_n	molar polarizability of nitrogen, $\text{cm}^3 \cdot \text{mol}^{-1}$
A_w, B_w	Debye constants describing the molar polarizability of water, $A_w + B_w/T$, $\text{cm}^3 \cdot \text{mol}^{-1}$
B_{nn}	nitrogen second virial coefficient, $\text{cm}^3 \cdot \text{mol}^{-1}$
B_{ww}	water second virial coefficient, $\text{cm}^3 \cdot \text{mol}^{-1}$
B_{nw}	nitrogen-water second virial coefficient, $\text{cm}^3 \cdot \text{mol}^{-1}$
B_{mix}	second virial coefficient of the gas mixture, $\text{cm}^3 \cdot \text{mol}^{-1}$
$\varepsilon = \varepsilon' - i\varepsilon''$	dielectric constant
f	resonance frequency of the RF resonator hygrometer, Hz
L	length of capillary, m
P	pressure, Pa
P_1	pressure at the capillary entrance, Pa
P_0	pressure at the capillary exit, Pa
Q_m	mass flow rate, $\text{kg} \cdot \text{s}^{-1}$
r	inner radius of capillary tube, m
R	gas constant, $\text{J} \cdot \text{mol}^{-1} \text{K}^{-1}$
s	quantity $(\varepsilon' - 1)/(\varepsilon' + 2)$
T	temperature, K
T_c	temperature of capillary, K
x_w	mole fraction of water
η	viscosity, $\text{Pa} \cdot \text{s}$

References

1. A. Mawardi, F. Yang, R. Pitchumani, *J. Fuel Cell Sci. and Tech.*, **2**, 121 (2005)
2. W. Wagner and A. Pruss, "The IAPWS Formulation 1995 for the Thermodynamic Properties of Ordinary Water Substance for General and Scientific Use," *J. Phys. Chem. Ref. Data*, **31**, 387-535 (2002).
3. P. H. Huang, D. C. Ripple, M. R. Moldover, G. E. Scace, "A Reference Standard for Measuring Humidity of Air Using a Re-entrant Radio Frequency Resonator," in Proc. 5th International Symposium on Humidity and Moisture (ISHM 2006), Rio de Janeiro, Brazil.
4. N. P. Cheremisinoff, *Fluid Flow: Pumps, Pipes and Channels*, (Ann Arbor Science, Ann Arbor, Michigan, 1981)
5. D. J. Tritton, *Physical Fluid Dynamics*, (Oxford University Press, 2nd Ed., 1988)
6. A. D. Buckingham, R. E. Raab, *Trans. Faraday Soc.* **54**, 623 (1958)
7. A. H. Harvey, E. W. Lemmon, *Int. J. Thermophys.* **26**, 31 (2005)
8. M. R. Moldover, T. J. Buckley, *Int. J. Thermophys.* **22**, 859 (2001)
9. G. Birnbaum, S. K. Chatterjee, *J. Appl. Phys.* **23**, 220 (1952)
10. J. H. Dymond and E. B. Smith, *The Virial Coefficients of Pure Gases and Mixtures, A Critical Compilation*, (Oxford Univ. Press, 1980)
11. A. H. Harvey, E. W. Lemmon, *J. Phys. Chem. Ref. Data* **33**, 369 (2004)
12. P. E. Huang, A. H. Harvey, NIST, private communication.

Table 1 Values and standard uncertainty values for example in Fig. 1.

Parameter	Value	Standard uncertainty	Notes
s	0.00267 to 0.0186	7×10^{-7}	
P	1.6 MPa	200 Pa	
T	473 K	0.2 K	(a)
A_n	$4.3901 \text{ cm}^3 \cdot \text{mol}^{-1}$	$3 \times 10^{-4} \text{ cm}^3 \cdot \text{mol}^{-1}$	
$A_w + B_w/T$	$47.9 \text{ cm}^3 \cdot \text{mol}^{-1}$	$0.28 \text{ cm}^3 \cdot \text{mol}^{-1}$	(b)
B_{ww}	$-203 \text{ cm}^3 \cdot \text{mol}^{-1}$	$4.1 \text{ cm}^3 \cdot \text{mol}^{-1}$	
B_{nn}	$14.7 \text{ cm}^3 \cdot \text{mol}^{-1}$	$1 \text{ cm}^3 \cdot \text{mol}^{-1}$	
B_{nw}	$-2.9 \text{ cm}^3 \cdot \text{mol}^{-1}$	$1.1 \text{ cm}^3 \cdot \text{mol}^{-1}$	

^a includes temperature non-uniformity of resonator

^b A_w, B_w statistically correlated

Figure Captions

Fig. 1. Schematic diagram of the generator. P indicates a pressure gauge; R indicates a pressure regulator; MFC indicates a mass flow controller. Thermometers are not indicated.

Fig. 2. Time stabilization of resonance frequency f in RF cavity for $T = 393.55 \text{ K}$, $x_w = 0.1816$, and $P = 0.4573 \text{ MPa}$.

Fig. 3. Resonance measurement of the RF resonator hygrometer for $T = 393.55 \text{ K}$, $x_w = 0.1816$, and $P = 0.5072 \text{ MPa}$: a) solid symbols are the in-phase data; open symbols are the quadrature data, and lines represent the fit; b) residuals to the fit.

Fig. 4. Significant uncertainty components and combined standard uncertainty for $T = 473 \text{ K}$ and $P = 1.6 \text{ MPa}$.

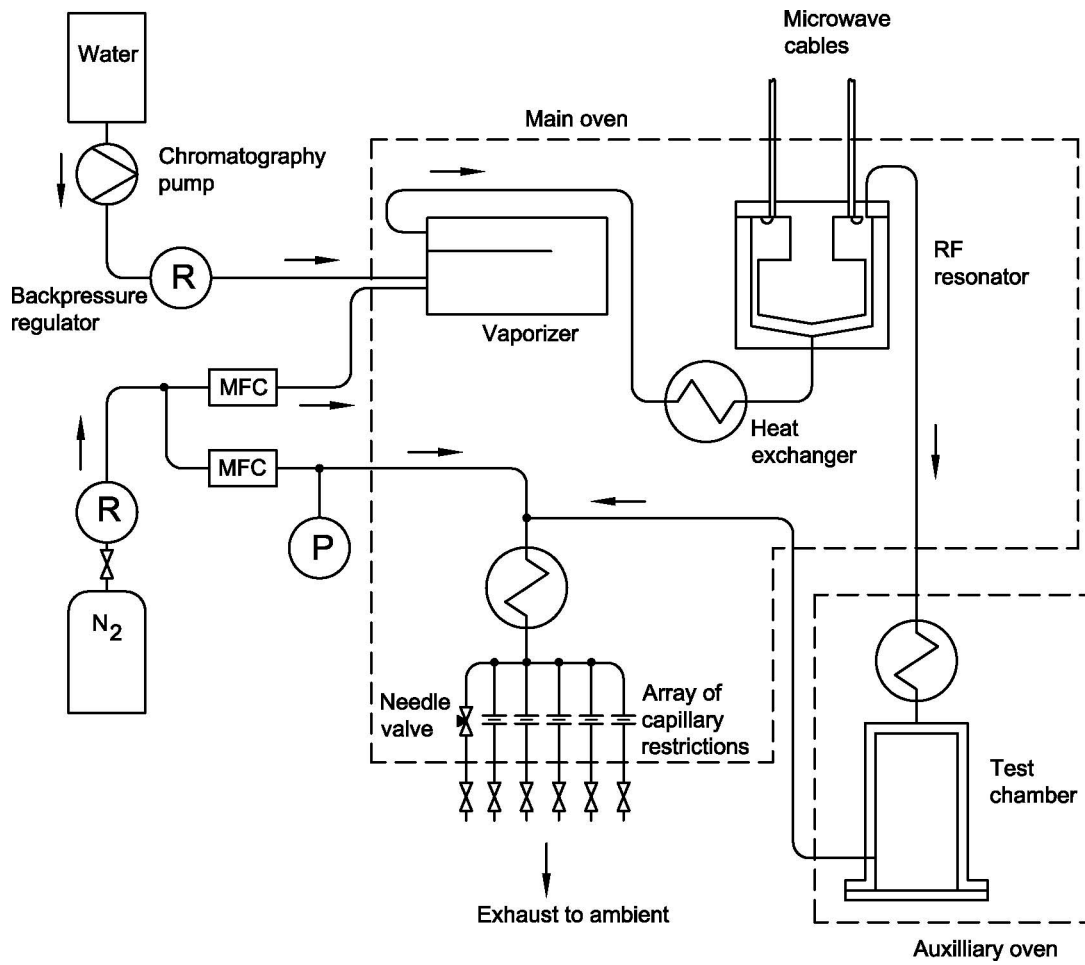


Fig. 1

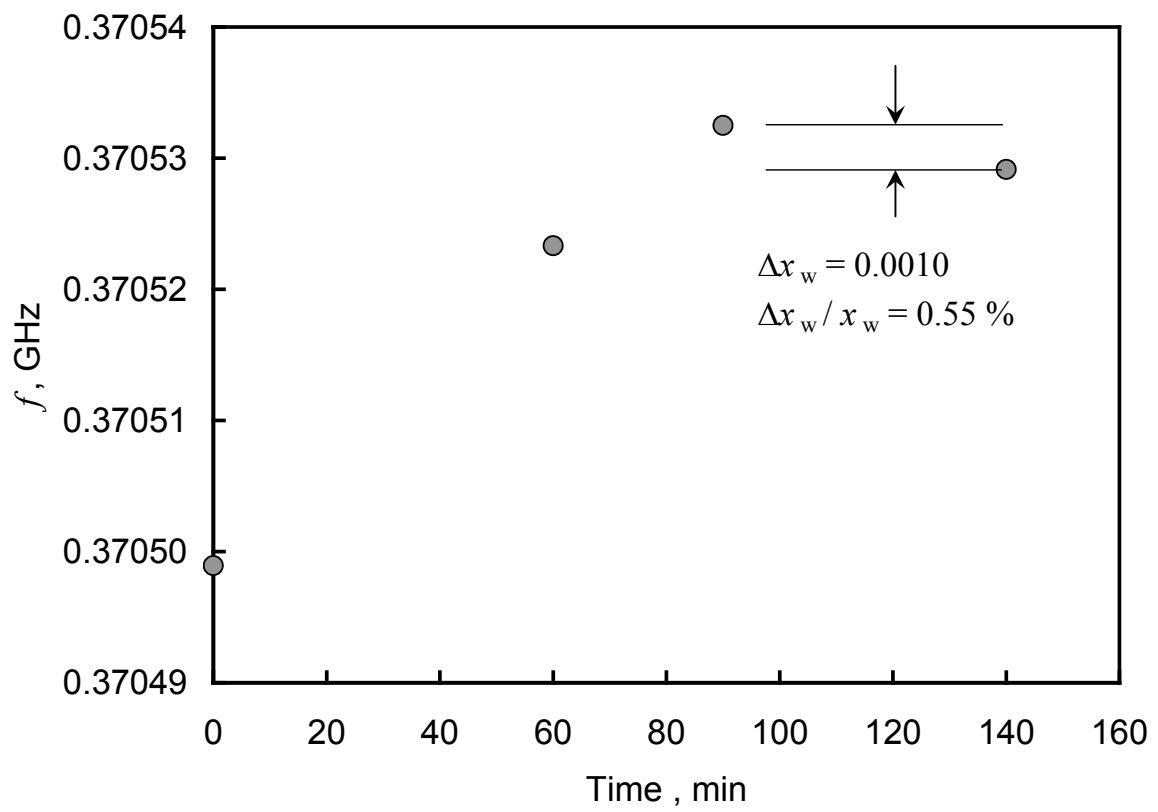


Fig. 2

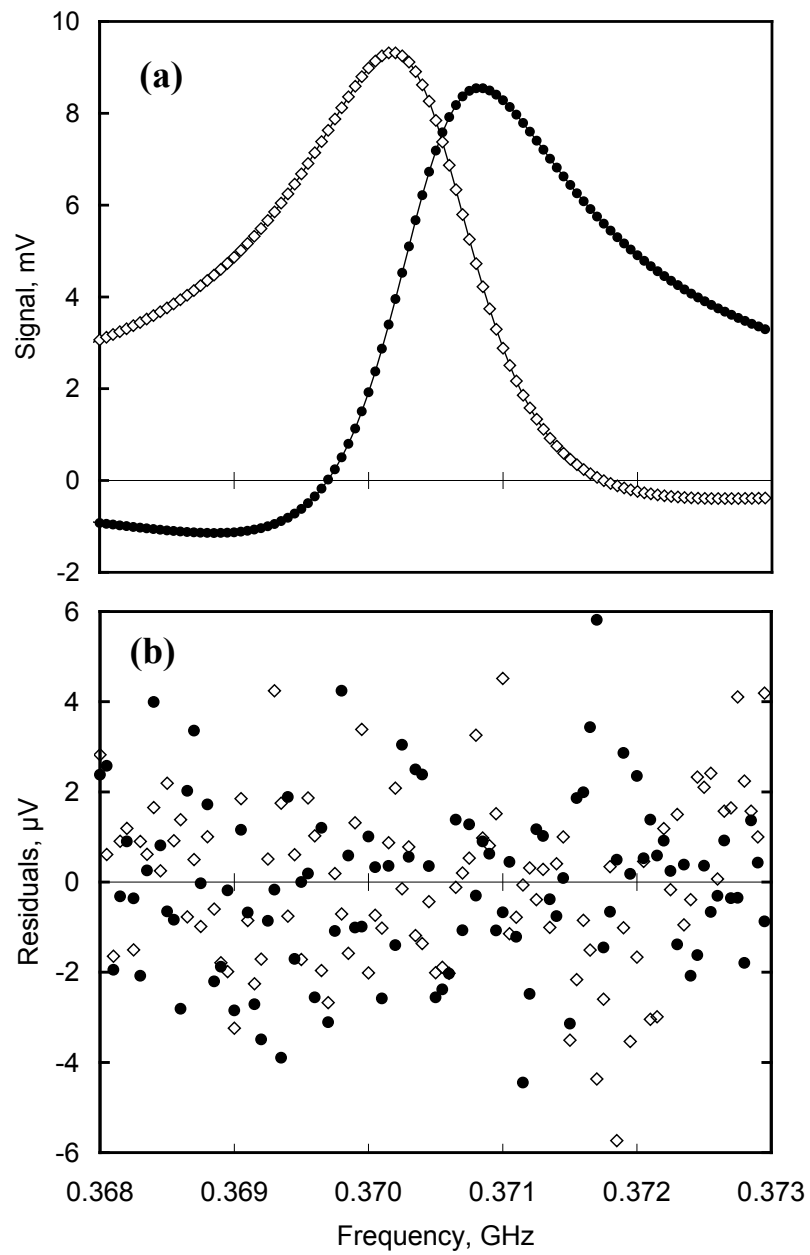


Fig. 3

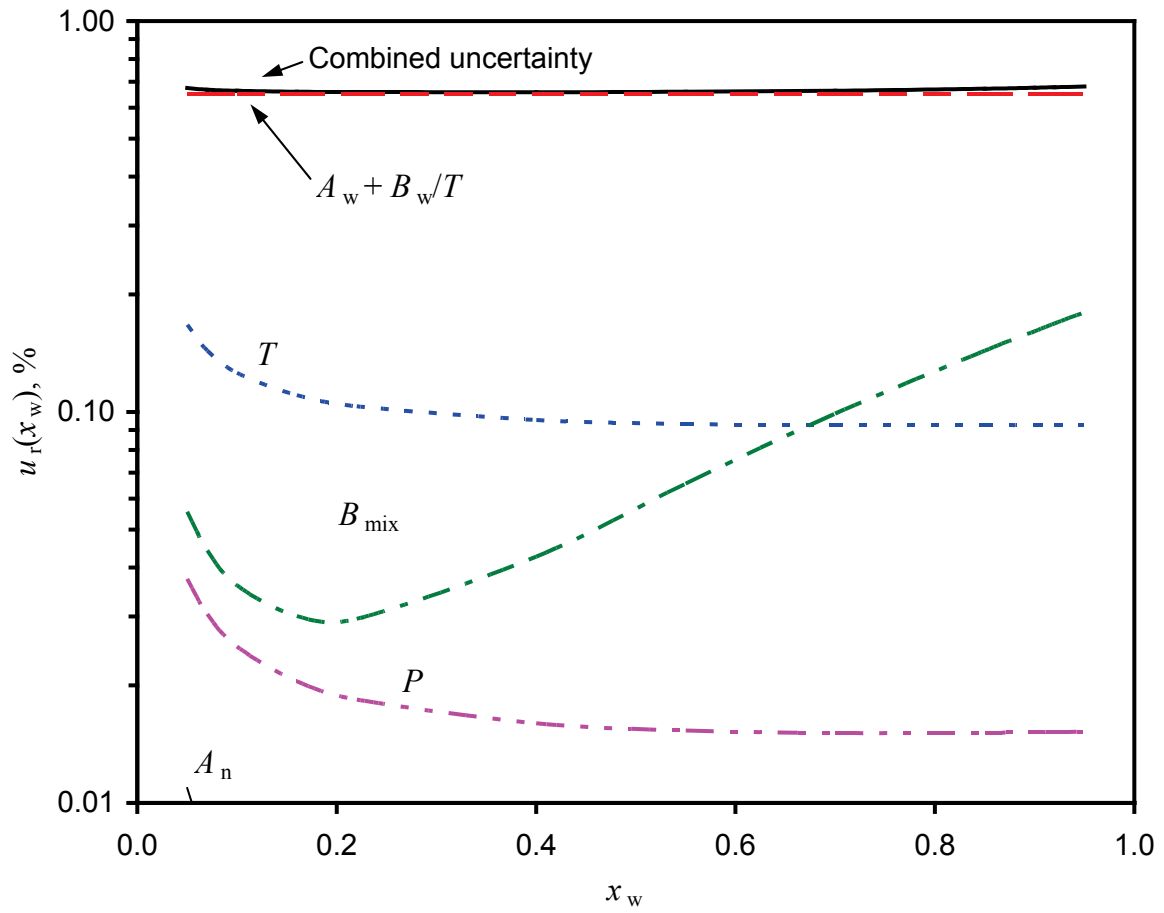


Fig. 4